Calculation of Heave of Deep Pier Foundations

J.D. Nelson[1], K.C. Chao[2], D.D. Overton[3], and R.W. Schaut[4]
[1]*Engineering Analytics, Inc., Fort Collins, Colorado, USA, jnelson@enganalytics.co*
[2]*Engineering Analytics, Inc., Fort Collins, Colorado, USA, gchao@enganalytics.com*
[3]*Engineering Analytics, Inc., Fort Collins, Colorado, USA, doverton@enganalytics.com*
[4]*Engineering Analytics, Inc., Fort Collins, Colorado, USA, rschaut@enganalytics.com*

ABSTRACT: Design of pier and grade beam foundations in highly expansive soils is one of the most important and challenging aspects of geotechnical engineering. Existing design methods consider only uniform soil profiles, and piers with limited length to diameter ratios. These methods are restricted with regard to evaluation of more complex aspects of pier heave. A finite element method of analysis was developed to compute pier movement in expansive soils having variable soil profiles, complex wetting profiles, large length-to-diameter ratios, and complex pier configurations and materials. The model has been named APEX (for Analysis of Piers in EXpansive soils). This paper describes the method of analysis and demonstrates its validity using several case histories. The results of pier design using APEX are compared with those of both conventional rigid pier analyses and elastic pier analyses. A series of simplified design charts developed using APEX are presented to facilitate its use. The results show the versatility of the model with regard to variable soil profiles and wetting zones.

1. INTRODUCTION

Foundations on expansive soils pose a unique challenge to the geotechnical engineer. They almost always cost more than foundations on ordinary soils, and the site investigation and foundation design costs more as well.

The Expansion Potential, EP, of an expansive soil is defined on the basis of percent swell exhibited in a consolidation-swell test and the swelling pressure of the soil (Nelson et al., 2007). For sites having a low to moderate EP, a variety of foundation systems have been proposed and used. However, for sites with high to very high expansion potential the most reliable method for foundation design is the use of pier and grade beam foundations. The grade beam forms a structural member of the foundation and must be designed to mitigate the effects of differential pier movement on the superstructure. The grade beam may be in the form of a reinforced basement wall or a stiff beam supported by the piers. Thus, an important part of the design of the foundation is the calculation of the heave of the individual piers.

Few methods have been developed to enable the calculation of pier heave. A readily available one is presented in Nelson and Miller (1992). It is based on finite element analyses by Poulos and Davis (1980). This method, however, was developed for uniform soil profiles and piers with limited length to diameter ratios. This method is limited in its application to more complex soil profiles and pier geometry. More recently a finite element method of analysis was developed to compute pier movement in expansive soils having variable soil profiles, complex wetting profiles, large length-to-diameter ratios, and complex pier configurations and materials. The model has been named APEX (for Analysis of Piers in EXpansive soils). This paper describes that model and demonstrates its validity using case histories. The results of pier design computations using the APEX model are compared with those of both conventional rigid pier analyses and elastic pier analyses. A series of simplified design charts developed using APEX are presented to facilitate its use. The results show the versatility of the model with regard to variable soil profiles and wetting zones.

2. FREE-FIELD HEAVE PREDICTION

Free-field heave is the fundamental parameter on which pier heave is calculated. Therefore, a review of free-field heave calculation will be presented first.

Free-field heave is the heave that will occur at the surface of a soil profile if no surcharge or stress is applied (Nelson and Miller, 1992). Methods for calculating free-field heave have been developed that use either oedometer tests or soil suction tests. The authors believe that the method based on oedometer test results has particular advantages, and that is the method used in this paper.

2.1 Prediction of free-field heave by oedometer method

A method for prediction of free-field heave using oedometer test data was outlined in Nelson and Miller (1992). A refinement of that method is presented in Nelson et al. (2006) and was presented in a panel discussion at the UNSAT 2010 conference (Nelson, 2010). The general equation for heave of a soil layer of thickness, Δz_i, is:

$$\rho = C_H \Delta z_i \log\left(\frac{\sigma'_f}{\sigma'_{cv}}\right)_i \tag{1}$$

where: ρ = free-field heave,
C_H = heave index,
σ'_f = in-situ effective stress state,
σ'_{cv} = swelling pressure from the constant-volume oedometer test; and
Δz_i = layer thickness.

2.2 Determination of heave index, C_H

The heave index, C_H, can be determined from consolidation-swell test data along with data from constant-volume tests. Because, the constant-volume test data can be approximated from consolidation-swell test data, all of the soil property data that is needed can be obtained from that test alone.

An example of consolidation-swell test data is shown in Figure 1. The slope of the loading portion of the curve shown in Figure 1 is the compression index, C_c, and that of the rebound portion of the curve is the rebound index, C_s. The volumetric strain experienced during inundation is the percent swell, %S.

Figure 2 shows the vertical overburden stress at three different depths in a soil profile with similar soil throughout. At all points all samples are in a condition of zero lateral strain with a vertical overburden stress equal to σ'_{vo}. If a consolidation-swell test is conducted on a sample identical to that at depth, Z_A, at an inundation stress, $(\sigma'_i)_A = (\sigma'_{vo})_A$, the sample will swell by an amount $\%S_A$ as shown in Figure 3. Similarly, for a sample at depth Z_B, the sample would be subjected to an inundation stress, $(\sigma'_i)_B = (\sigma'_{vo})_B$, and the sample would swell by an amount $\%S_B$. Obviously, if a sample is tested at an inundation pressure equal to the constant-volume swelling pressure, σ'_{cv}, the sample will not swell and the test data would define point C in Figure 3.

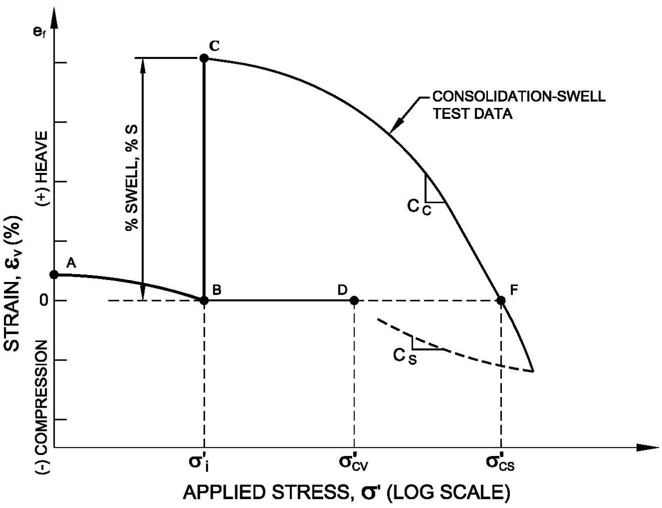

Figure 1 Terminology and notation for oedometer tests

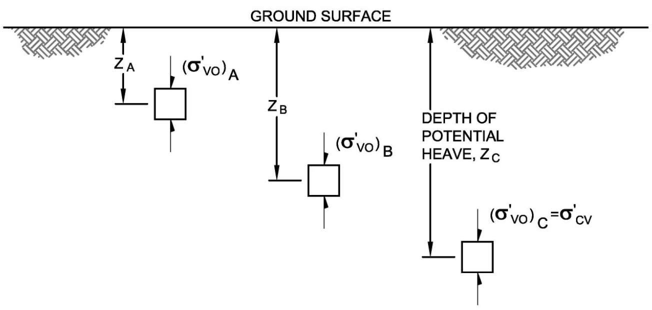

Figure 2 Vertical stress states in soil profile

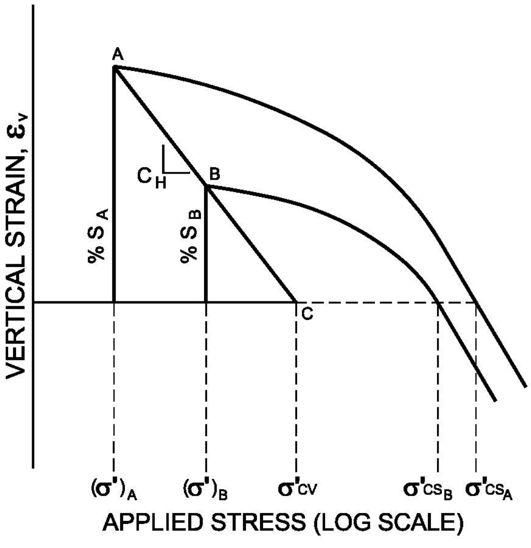

Figure 3 Hypothetical oedometer test results for stress states shown in Figure 2

To arrive at the form of Equation (1), it is convenient to start with the general equation for heave in a soil stratum of thickness, Δz. That is,

$$\rho = \varepsilon_v \cdot \Delta z_i = \%S \cdot \Delta z_i \tag{2}$$

For a layer of thickness, Δz, the overburden pressure and applied stress will influence the amount of swell that will occur when that layer becomes wetted. Because that stress varies from layer to layer, it is necessary to define a relationship between the amount of swell that occurs and the imposed stress when the soil is wetted, i.e., the inundation pressure. That relationship is defined by the line ABC in Figure 3. For practical purposes, the line ABC can be defined by a straight line connecting point A (the point defined by the percent swell in a consolidation-swell test) and point C (the point corresponding to the constant volume swell pressure, σ'_{cv}. The slope of that line is denoted by the heave index, C_H, where:

$$C_H = \frac{\%S_A}{\log\sigma'_{cv} - \log(\sigma'_i)_A} = \frac{\%S_A}{\log\left[\dfrac{\sigma'_{cv}}{(\sigma'_i)_A}\right]} \tag{3}$$

If values of C_H and σ'_{cv} are known, the vertical strain, or percent swell, that will occur during inundation at any depth z in a soil profile can be determined from Equation (3). For the case of free field heave when the soil at depth z is inundated, the stress on the soil is the overburden stress, $(\sigma'_{vo})_z$. This value is, therefore, the inundation stress, σ'_i, in the field and Equation (3) can be rewritten as Equation (4).

$$(\varepsilon_v)_z = \%S_z = C_H \log\left[\frac{\sigma'_{cv}}{(\sigma'_{vo})_z}\right] \tag{4}$$

Therefore, for a layer of soil of thickness, Δz_i that exists at a depth z to its midpoint, the maximum heave that will occur due to expansion of that stratum during complete inundation would be obtained by substituting Equation (4) into Equation (2). Thus,

$$\rho_{oi} = C_H \cdot \Delta z_i \log\left[\frac{\sigma'_{cv}}{(\sigma'_{vo})_z}\right] \tag{5}$$

In actual application of Equation (5), a soil profile will be divided into layers of thickness, Δz, the value of heave for each layer will be computed, and the incremental values will be added to determine the total heave. It should be noted that the value of $(\sigma'_{vo})_z$ to be used in Equation (5) is the stress at the midpoint of the layer at depth z. In a soil with no applied load, that value would be the overburden pressure. If a load is applied to the soil, for example, by a footing or stiffened slab, the value of $(\sigma'_{vo})_z$ to be used in Equation (5) is the overburden stress plus the applied stress.

The line ABC in Figure 3 and the heave index, C_H, can be determined by conducting consolidation-swell and constant volume oedometer tests on samples of the same soil and connecting point A obtained from the consolidation-swell test with point C obtained from the constant volume test. However, to do so is generally not practical, mainly because it is almost impossible to obtain two identical samples from the field. A relationship between σ'_{cv} and σ'_{cs} has been proposed so that the value of the heave index can be determined from a single consolidation-swell test (Nelson et al., 2006).

Method A in the ASTM D4546-08 Standard consists of performing oedometer tests on four different samples of soil. Each sample is inundated at a different applied stress and the percent swell, S%, is plotted against the inundation stress. Figure 4 shows the data for Method A that is plotted in the ASTM Standard. It is normal to plot oedometer test that results in semi-logarithmic form. Figure 5 shows the Method A data from the ASTM Standard plotted in semi-logarithmic form. It is seen that the data plots as a straight line. Therefore, the Method A presented in the ASTM Standard is identically the same as that shown in Figure 3 for predicting heave. This lends credibility to considering line ABC in Figure 3 as a straight line.

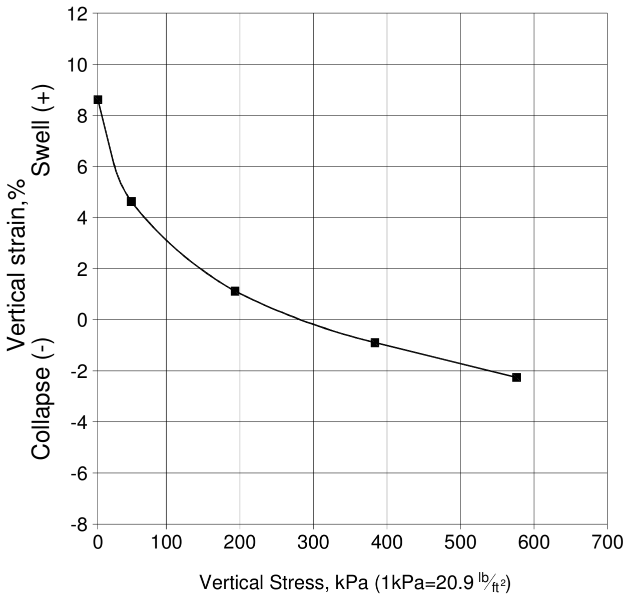

Figure 4 Data from Method A of the ASTM D4546-08 Standard

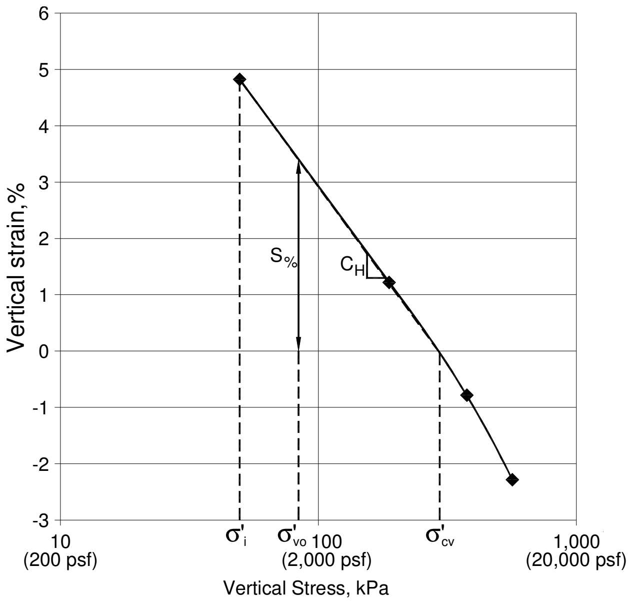

Figure 5 Method A data from the Standard plotted in semi-logarithmic form

2.3 Relationship between σ'_{cv} and σ'_{cs}

Nelson et al. (2006) proposed a relationship between the constant-volume swelling pressure, σ'_{cv}, and the consolidation-swell swelling pressure, σ'_{cs}, in an arithmetic form as follows:

$$\sigma'_{cv} = \sigma'_i + \lambda(\sigma'_{cs} - \sigma'_i) \tag{6a}$$

The rationale behind this equation is that the value of σ'_i must be less than σ'_{cv}, otherwise heave would not have occurred. Also it is reasonable to expect that σ'_{cv} will be less than σ'_{cs}. Equation (6a) proposes that the value of σ'_{cv} falls between σ'_i and σ'_{cs} by the proportionality defined by the value of λ. Nelson et al. (2006) indicated that a reasonable value for λ is 0.6 for the clay soil in the Front Range area of Colorado, USA. They concluded that since the value of λ is dependent upon mineralogy of the clay soil, the λ value should be determined for soil on a regional basis.

The authors recently analyzed additional swelling pressure data determined from the consolidation-swell tests and constant-volume tests and proposed a new relationship between σ'_{cv} and σ'_{cs} in a logarithmic form as shown in Equation (6b). The swelling pressure data used for this analysis were obtained from literature (Porter, 1977; Reichler, 1997; Feng et al., 1998; Bonner, 1998; Fredlund, 2004; Thompson et al. 2006; and Al-Mhaidib, 2006). The types of the soils collected from the literature include claystone, weathered claystone, clay, clay fill, and sand-bentonite.

$$\log \sigma'_{cv} = \log \sigma'_i + \lambda(\log \sigma'_{cs} - \log \sigma'_i) \tag{6b}$$

The λ values determined using Equation (6b) range from 0.36 to 0.90 with an average value of 0.62 for the claystone and range from 0.36 to 0.97 with an average value of 0.59 for all soil types. Figure 6 shows the histograms of the ranges of the λ values for the claystone and all soil types, respectively. Figure 6 shows that the λ value could vary even for the same soil type, which confirms the conclusion described above by Nelson et al. (2006).

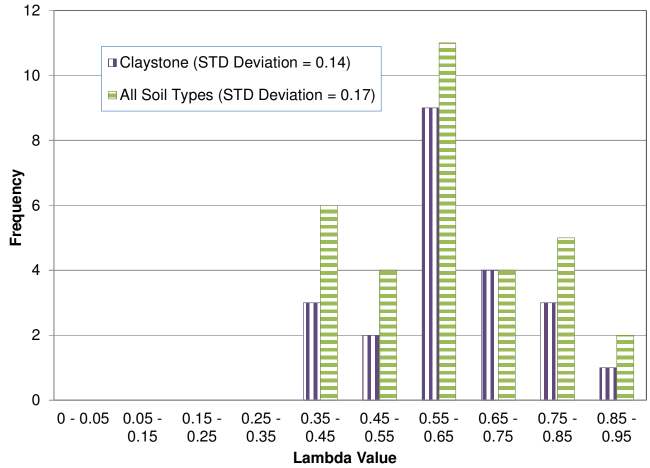

Figure 6 Histograms of the λ values determined using the logarithmic form for the claystone and all soil types

2.4 Depth of wetting / degree of wetting

The depth of soil that is contributing to heave at a particular point of time depends on two factors. These are the depth to which water contents in the soil have increased since the time of construction, and the expansion potential of the various soil strata. As water migrates through a soil profile different strata become wetted, some of which may have more swell potential than others. Consequently, the zone of soil that is contributing to heave varies with time.

The amount of heave that will occur at a particular time depends on the manner in which the groundwater migrates in the soil and the expansion potential of the soil at depth. Movement of the soil surface will begin almost immediately after construction, whereas some time will be required for the soil at deeper depths to become wetted. Thus, the surface of the soil will begin to heave almost immediately, but movement of piers will be delayed, sometimes by several years.

The term "active zone" has been in common usage in the field of expansive soils. However, the usage of that term has taken different meanings at different times and in different places. Therefore, for purposes of clarity and consistency, the following five definitions have been put forth (Nelson et al., 2001).

<u>Active Zone</u>, Z_A, is that zone of soil that is contributing to heave due to soil expansion at a particular point in time. The depth of the active zone will vary as heave progresses, and therefore, it varies with time.

<u>Zone of Seasonal Moisture Fluctuation</u>, Z_s, is that zone of soil in which water contents change seasonally due to climate changes.

<u>Zone of Wetting</u>, Z_w, is that zone in which water contents have increased over the pre-construction equilibrium conditions. Factors contributing to this could include capillary rise after the elimination of evapotranspiration from the surface, infiltration due to irrigation or precipitation, or introduction of water from off-site. Underground

sources may include broken water lines, development of perched water tables, or flow through permeable strata that are recharged at distant locations.

Depth of Potential Heave, Z_p, is the depth to which the overburden vertical stress equals or exceeds the swelling pressure of the soil. This represents the maximum depth of the active zone that could occur.

Design Active Zone, Z_{AD}, is the active zone for which the foundation is designed. This is the zone of soil that is expected to have become wetted during the design life. It may be less than the depth of potential heave if water migration analyses indicate that the entire depth of potential heave will not become wetted. If water migration analyses are not available and if the depth of potential heave is of reasonable value for design, it is prudent to assure the designative zone is equal to the depth of potential heave.

2.4.1 Saturated water content profile

Construction of buildings and pavements in arid regions typically results in a reduction of evapotranspiration from the soil. Additionally, the introduction of irrigation typically exceeds the evapotranspiration of the vegetation. These factors as well as others result in the development of a wetting front that progresses downward in the soil. Below the wetting front the water content is the same as that which existed prior to introduction of the water source. However, above the wetting front the water contents are higher, and the soil may be saturated or unsaturated. The difference in soil suction between the wetter and drier zones will result in downward flow of water, and the wetting front will continue to move downward until an impermeable boundary or a water table is reached (McWhorter and Nelson, 1979). Once an impermeable boundary is reached, the water table will propagate upward to the surface, thusly, forming a perched water table. Full wetting of the soil profile would be expected to occur if the soil above the wetting front is saturated and the wetting front advances to below the depth of potential heave. Where a rising groundwater table is anticipated, the full wetting conditions should be used to make calculations (Houston et al., 2001).

If full wetting is not expected to occur, analyses must be conducted to determine the water content profile at the end of the design life. If such analyses are not conducted it should be assumed that full wetting will occur to below the depth of potential heave.

2.4.2 Vadose zone modelling

For sites at which the depth of potential heave is large, the degree of wetting typically will be less than fully saturated (Chao et al., 2006; Overton et al., 2006). Design of foundations for these conditions must consider the design life of the structure, the depth of wetting that can occur during the design life, and the degree of saturation, and thus the portion of potential heave that can develop during the design life.

The depth of wetting and corresponding degree of saturation can be calculated using readily available software, such as Vadose/W, SVFlux, or Hydrus 2-D. Using the results of these analyses, the amount of heave that is expected to occur in the partially wetted zone can be calculated. This amount of heave will be less than that calculated assuming full wetting for the entire depth of potential heave.

Example results of the analysis of wetting due to irrigation and precipitation are shown in Figure 7. Analyses were conducted using the computer program Vadose/W (GEO-SLOPE, 2007). Vadose/W can model both saturated and unsaturated flow in response to climatic and environmental conditions, making it possible to analyze water migration as a function of time. The program considers the effect of precipitation and infiltration, surface seepage, runoff and ponding, plant transpiration, potential and actual evaporation, snow accumulation and melt, ground freezing and thawing, and groundwater recharge.

A one-dimensional profile that consisted of homogeneous claystone was used for this example. Actual site data were used in the analysis. These included initial water contents prior to development, post-development irrigation values, and climate data. Climate data were generated using the ClimGen program (Washington State University, 2002) based on 20 years of historical data from a nearby NOAA certified weather station. The soils properties used in the analyses are presented in Table 1.

Table 1 Soil properties for claystone

Saturated hydraulic conductivity, K_v (cm/sec)	2.0×10^{-8}
Porosity, n	0.37
Displacement pressure, h_d (m)	30
Pore size distribution index, λ	0.218

The Vadose/W model was used to model a period of 100 years. The results of the analyses are shown on Figure 7. The volumetric water content of the claystone is predicted to increase up to about 32 percent near the ground surface. Wetting is predicted to occur to a depth of approximately 11 meters in 100 years.

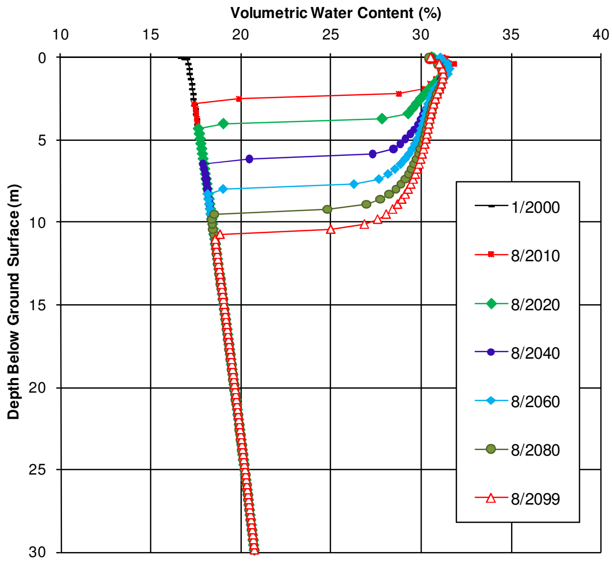

Figure 7 Water content profiles for claystone calculated by Vadose/W

2.4.3 Simplified hand calculations

McWhorter and Nelson (1979) developed a method of analysis to model the movement of the wetting front. Below the wetting front the pressure head in the soil is dictated by the soil suction, which in turn, is a function of the water content. They derived the following generalized relationship between the hydraulic conductivity and volumetric water content.

$$k_e = k_s \left(\frac{\theta_f - \theta_r}{n - \theta_r} \right)^{\frac{(2+3\lambda)}{\lambda}} \tag{7}$$

where:
k_e = effective hydraulic conductivity,
k_s = saturated hydraulic conductivity,
θ_f = final volumetric water content,
θ_r = residual volumetric water constant,
n = porosity, and
λ = pore size distribution index.

According to Darcy's law, for the case where water is continuously ponded to a small depth at the ground surface, the infiltration at the surface, q_i, in a homogeneous and isotropic medium is represented by Equation (8):

$$q_i = k_e\left(1+\frac{h}{z}\right) \tag{8}$$

in which h = pressure head and z = elevation head, and other symbols are as previously defined.

McWhorter and Nelson (1979) showed that a good approximation for the pressure head, h, at the wetting front is to assume that the suction is equal to the displacement pressure, h_d, of the soil. Assuming the pressure head due to the ponding at the surface is negligible, and that the wetting front has progressed to the depth of potential heave. Equation (8) can be expressed as follows:

$$q_i = k_e\left(1+\frac{h_d}{Z_p}\right) \tag{9}$$

The infiltration, q_i, does not completely contribute to downward migration of the wetting front. Some of it is retain in the pore spaces of the soil and increases the water content. This increase in water content is, of course, the factor that causes heave.

Combining Equations (7) and (9) yields,

$$\theta_f = \theta_r + \left\{(n-\theta_r)\left[\frac{q_i}{k_s}\left(\frac{Z_p}{Z_p+h_d}\right)\right]^{\frac{\lambda}{2+3\lambda}}\right\} \tag{10}$$

Equation (10) can be simplified for unsaturated clay soils as follows:

$$\theta_f = n\left[\frac{k(\theta_f)}{k_s}\left(\frac{Z_p}{Z_p+h_d}\right)\right]^{\frac{\lambda}{2+3\lambda}} \tag{11}$$

If $k(\theta_f) \le k_s$, Equation (11) can be further simplified as Equation (12).

$$\theta_f \le n\left(\frac{Z_p}{Z_p+h_d}\right)^{\frac{\lambda}{2+3\lambda}} \tag{12}$$

Calculations were performed for the homogeneous claystone profile that was discussed in Section 2.4.2. Using the soil properties presented in Table 1 and a value of Z_p of 19.1 meters presented in Table 2, the results of these analyses indicated that a final constant volumetric water content of 34% can be used for design. This result is compared with the Vadose/W results in Figure 8. It is seen that this is a conservative estimate for the wetting profile. However, it is less conservative than assuming fully saturated conditions.

Table 2 Claystone Parameters Used for Heave Prediction

Total Unit Weight	Percent Swell, S%	Swelling Pressure, σ'_{cs}	Heave Index, C_H	Depth of Potential Heave, Z_p
(Mg/m^3)	(%)	(kPa)		(m)
1.86	4.2	608	0.046	19.1

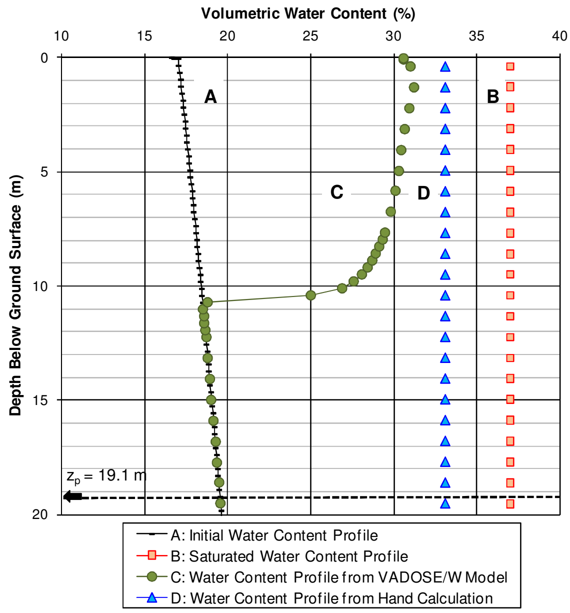

Figure 8 Comparison of design water content profiles

2.5 Rate of heave

The free-field heave of the soil for the saturated final water content, as discussed in Section 2.4.1, was calculated using Equation (5). The calculations result in 384 mm of predicted free-field heave. The soil parameters used for the analyses are presented in Table 2.

The final water content profile calculated by the Vadose/W program and that calculated using Equation (12) as presented in Figure 8 were also used to calculate the free-field heave.

For soils that are not fully wetted, the percent swell and the swelling pressure will be less than that measured after saturation in the consolidation–swell test. Therefore, in calculating heave those values must be corrected for the actual degree of saturation. Normalized degree of saturation versus the normalized percent swell for initial degree of saturation of 42, 52, 66, and 84 percent, are shown in Figure 9 (Chao, 2007). These curves can be used to calculate the percent swell for a non-fully wetted soil.

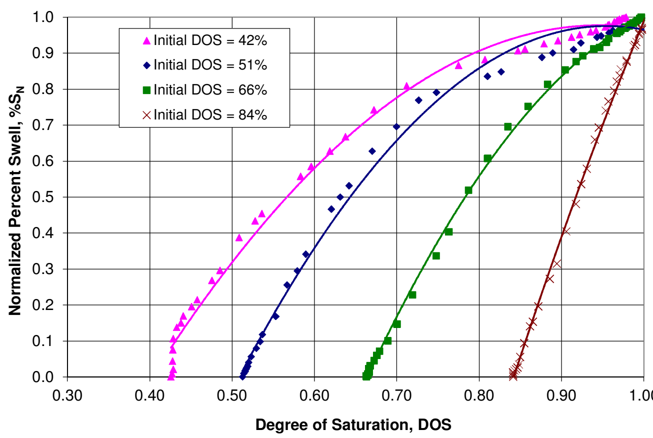

Figure 9. Normalized percent swell vs. degree of saturation (modified from Chao, 2007)

The swell pressure can be corrected in a similar fashion. Reichler (1997) showed that an e-log p curve from a partially saturated consolidation-swell test has the same shape as that from a fully wetted consolidation-swell test.

Using the revised percent swell as calculated in the above discussion, the consolidation-swell line can be shifted downward parallel to the fully wetted line and the corrected value of swell pressure for the partially wetted soil can be calculated. The values of normalized degree of saturation for the Vadose/W water content profile are presented in Table 3. The calculated free-field heave using this methodology was 287 mm for the water content profile in 100 years obtained from the Vadose/W program.

Using the final design volumetric water content of 33 percent that was determined using Equation (11), and the method presented above for calculation of heave for partially saturated soils, the calculated free-field heave was 362 mm.

The calculated values of free-field heave for the three scenarios of wetting are compared in Table 4. The Vadose/W value is 25 percent less than that for the fully wetted condition whereas the hand calculation is only 6 percent less. For a more permeable soil, however, there would be a greater difference for the hand calculation.

Table 3 Normalized Final Degree of Saturation from Vadose/W Model

Depth (meters)	Normalized Final Degree of Saturation
0 - 2	0.94
2 - 4	0.94
4 - 6	0.92
6 - 8	0.90
8 - 10	0.85
10 - 12	0.24

Table 4. Calculated values of free field heave

Water Content Profile	Free-Field Heave (mm)
Saturated Profile	384
Vadose/W	287
Simple Hand Calculation	362

3. PIER HEAVE PREDICTION

Figure 10 shows a pier and grade beam foundation system in which the basement wall serves as the grade beam. A void space must be maintained between the grade beam so that as the soil heaves it will not exert uplift forces on the grade beam and piers.

Piers can be of different types. They may be straight shaft drilled piers, they may be drilled piers with belled ends, they may be steel piles that are driven or pushed, they may be helical piers, or they may be micropiles. The principle on which the piers are designed is to found them in a sound stratum at sufficient depth so as to provide sufficient anchorage to minimize movement under the uplift forces exerted by the expansive soil.

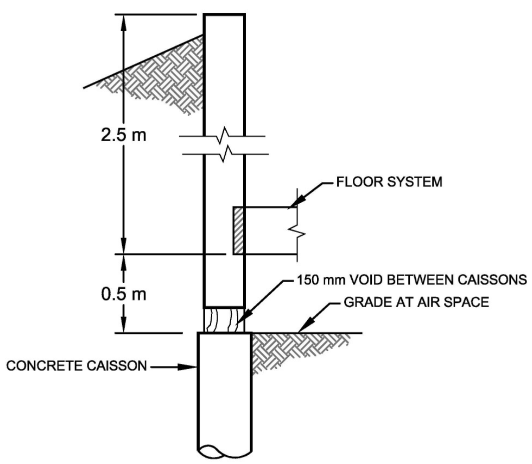

Figure 10 Typical pier and grade beam foundation system

If a stable non-expansive stratum exists sufficiently near the surface, the pier may be designed as a rigid body anchored in the soil stratum so as to prevent movement. With rigid pier design, it is assumed that the pier does not move.

If the design depth of active zone is large, the design length of a pier designed as a rigid pier will be too long to be practical. In design of most structures, however, some movement of the pier would be tolerable. Economic design of the pier would be to calculate the required length of pier such that the tolerable movement is not exceeded. The pier should then be designed as an elastic member in an elastic medium. The methods for design of a rigid pier and for calculating heave of an elastic pier are presented below.

3.1 Rigid pier analysis

Rigid pier design is presented in Chen (1988). The forces acting on a rigid pier in expansive soil are shown in Figure 11. The principle of the design is that the negative skin friction below the depth of potential heave plus the dead load, P, must resist the uplift pressures produced by the swelling pressures exerted on the pier above that point.

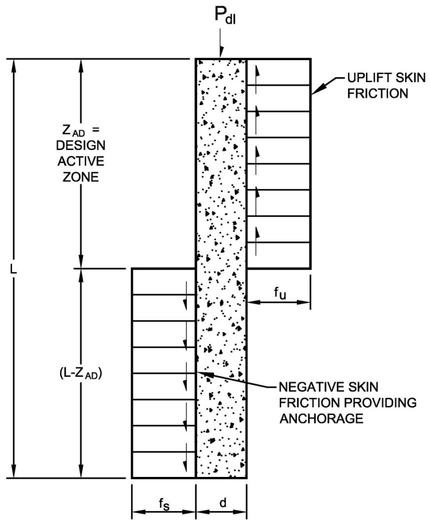

Figure 11 Forces acting on a rigid pier

The equation for required length of a rigid straight shaft pier as presented in Nelson and Miller (1992) is,

$$L = Z_{AD} + \frac{1}{f_s}\left[\alpha_1 \sigma'_{cv} Z_{AD} - \frac{P_{dl}}{\pi d}\right] \tag{14}$$

where:
- Z_{AD} = the depth of the design active zone,
- f_s = the negative skin friction below the depth of potential heave,
- α_1 = a coefficient of adhesion between the pier and the soil,
- σ'_{cv} = the swelling pressure from the constant volume pressure;,
- P_{dl} = dead load on the pier, and
- d = diameter of the pier.

The maximum tensile force generated in the pier, P_{max}, will occur at the bottom of the depth of design active zone and will be equal to

$$P_{max} = P_{dl} - f_u Z_{AD} \pi d \tag{15}$$

where f_u = the uplift skin friction = $\alpha_1 \times \sigma'_{cv}$ and all other terms were defined in Equation (14).

A more complete treatment of rigid pier design is presented in Nelson and Miller (1992).

Rigid pier design works well if the stratum of expansive soil is not thick and is underlain by a stable non-expansive stratum. However, in a deep deposit of expansive soil, the required pier length approaches a value equal to twice the depth of potential heave. In such cases the design rigid pier length is generally not practical for a light structure, and it would be appropriate to use a shorter pier designed according to elastic pier design.

3.2 Elastic pier analysis

Elastic pier design is presented in Nelson and Miller (1992). The heave prediction method for calculating pier heave, as presented therein, is based on a finite element solution for pier heave developed by Poulos and Davis (1980). The material presented by Poulos and Davis was modified by Nelson and Miller (1992) to make it more easily usable by the design engineer. The material below is modified further from Nelson and Miller (1992).

The uplift skin friction along the side of the pier may be considered to be uniform along the length of the pier or to increase with depth as shown in Figure 12. A uniform distribution would be assumed for the situation where the soil within the depth of the design active zone has generally the same swelling pressure throughout. A linearly increasing distribution would be appropriate for several strata of soils where the deeper soils exhibit a higher expansion potential.

Figure 12 shows normalized pier heave for a straight shaft pier plotted as a function of the pier length normalized against the depth of the design active zone for a straight shaft pier. Similar curves are presented in Figure 13 for belled piers having a bell diameter twice that of the shaft.

Figures 14 and 15 show the normalized maximum tensile force in straight shaft and belled piers plotted as a function of the pier length normalized against the depth of the design active zone. The maximum force is normalized to a force, P_{FS}, computed by applying the uplift friction over the entire length of the pier.

For the case where the skin friction varies linearly with depth, the force, P_{FS}, is equal to,

$$P_{FS} = -0.5 f_{um} L \pi d \tag{16}$$

For the case where the skin friction is uniform with depth, the force, P_{FS}, is equal to,

$$P_{FS} = -f_{um} L \pi d \tag{17}$$

3.3 APEX method

The elastic pier method is somewhat limited in that it considers only one soil throughout the depth of the pier, and it was developed for L/d ratios of about 20 or less. In many cases the various strata of expansive soil that are penetrated by the pier exhibit widely varying properties. Also, with increasing use of micropiles in expansive soil applications, L/d ratios well in excess of 20 are common. In order to provide for a more versatile method of analysis a finite element based model was developed. The code for that analysis is termed APEX for Analysis of Piers in EXpansive soils. The development of that code is presented below. A detailed description of the code is presented in Nelson et al. (2010). Design charts developed using that codes are demonstrated and an example is presented to illustrate the use of this method to analyse and design piers.

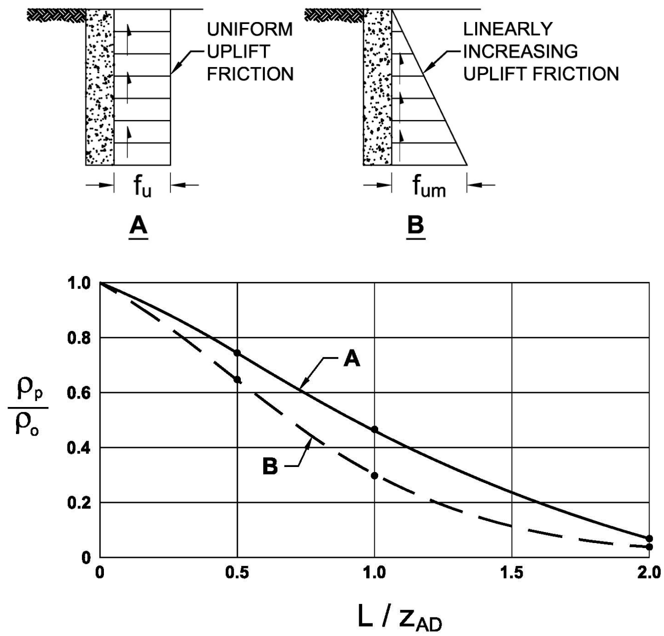

Figure 12 Normalized straight shaft pier heave vs. L/Z_{AD}

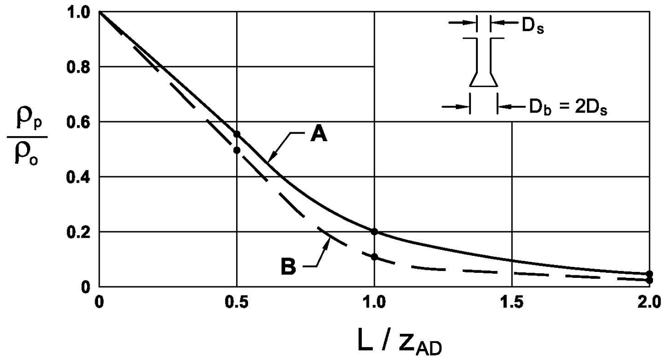

Figure 13 Normalized belled pier heave vs. L/Z_{AD}

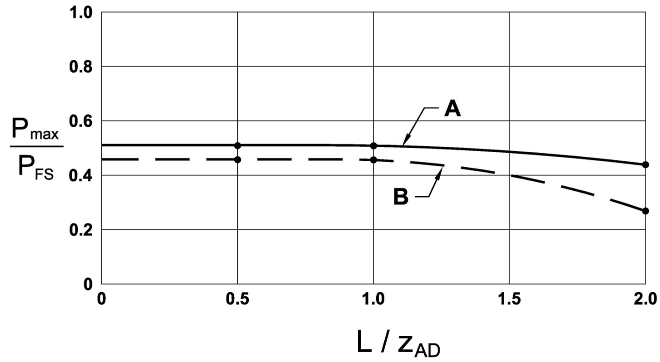

Figure 14 Normalized force in straight shaft piers vs. L/Z_{AD}

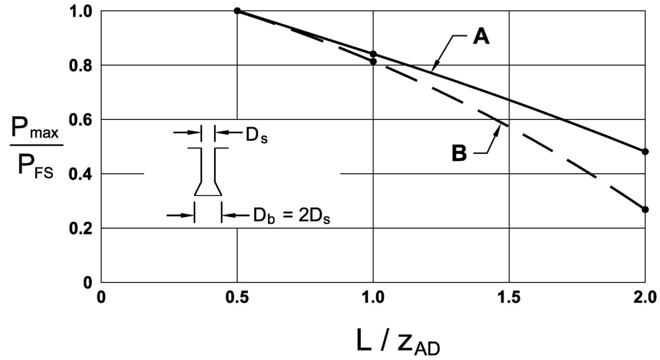

Figure 15 Normalized force in belled piers vs. L/Z_{AD}

3.3.1 The field equations with soil swelling

Material properties can be specified point-wise throughout the analysis domain. The swell is assumed to be isotropic and is accounted for by writing the constitutive equations as:

$$\varepsilon_{rr} = \frac{1}{E}\left[\sigma_{rr} - \nu\left(\sigma_{\theta\theta} + \sigma_{zz}\right)\right] + \varepsilon_{iso} \tag{18}$$

$$\varepsilon_{\theta\theta} = \frac{1}{E}\left[\sigma_{\theta\theta} - \nu\left(\sigma_{zz} + \sigma_{rr}\right)\right] + \varepsilon_{iso} \tag{19}$$

$$\varepsilon_{zz} = \frac{1}{E}\left[\sigma_{zz} - \nu\left(\sigma_{rr} + \sigma_{\theta\theta}\right)\right] + \varepsilon_{iso} \tag{20}$$

where: ε_{iso} = isotropic swelling strain,

ε_{rr}, $\varepsilon_{\theta\theta}$, ε_{zz} = components of stress and strain in cylindrical coordinates, and

E = modulus of elasticity of the soil.

3.3.2 The boundary conditions

The pier-soil interface must be modeled such that either slip between the soil and the pier (Coulomb friction) or failure within the soil adjacent to the pier (Mohr-Coulomb failure) can take place. Axial strain in the pier is assumed to be negligible relative to strain in the soil.

The boundary conditions at the pier-soil interface specify a relationship between the nodal displacement and nodal force, rather than the actual value of one or the other. In the APEX code, this specification is used for the vertical component of displacement at nodes where the soil would be in contact with the pier. It is shown schematically in Figure 16, and has the following form:

$$F_t = k(H_p - U_t) \tag{21}$$

where: F_t = the nodal force tangent to pier; H_p = the pier heave; U_t = the nodal displacement tangent to pier; and k = the parameter used to adjust shear stress, considered similar to a spring constant of the connection between U_t and H_p.

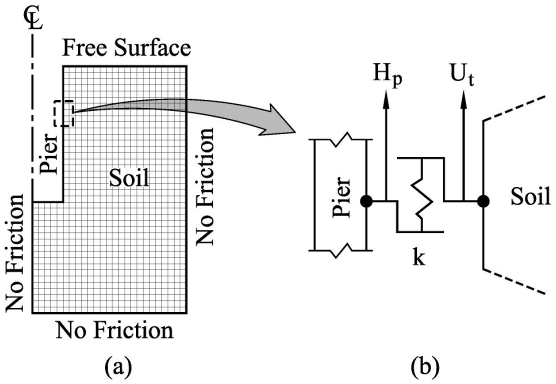

Figure 16. Boundary conditions: (a) soil boundary conditions, (b) pier-soil boundary condition

The pier heave (H_p) is assumed to be the same for all nodes because of the pier's rigidity. Large values of k require U_t to be approximately equal to H_p. In these cases, the soil has the same displacement as the pier. This no-slip condition is used as the initial condition for all such nodes. However, when the force at any node exceeds that necessary to cause either slip between soil and pier, or soil failure adjacent to the pier, k is reduced to bring the shear to its smallest allowable value. That value would be the smaller of either that which will cause slip, or that which will cause soil failure.

Limiting values for shear as defined by Coulomb friction (slip) and Mohr-Coulomb failure (soil failure) are in terms of normal and tangential components of stress. For computational efficiency, these relationships are converted to equivalent nodal forces with no loss in the generality of the theory. For the Mohr-Coulomb failure theory, it is also necessary to determine soil strain, which poses a unique problem which will be discussed as a separate issue.

3.3.3 Adjustment in pier heave

The pier must be in equilibrium, and therefore, the tangential forces exerted on the pier by the soil must equal the total external load on the pier. Figure 17 illustrates how H_p is adjusted in order to bring about equilibrium. Figure 17a illustrates the boundary conditions before the soil swells. In this state there is no uplift force on the pier. Figure 17b illustrates the state of the mixed boundary conditions after swelling takes place but before any pier heave. The shear forces create an upward force on the pier, and the pier is no longer in equilibrium (for simplicity, the pier is shown as having no external load). To bring the pier into equilibrium, it must be allowed to move up, creating both upward and downward forces acting on the pier. This is illustrated in Figure 17c. For given k values, the relationship between heave and total force is linear, thus this adjustment requires an insignificant amount of computer time.

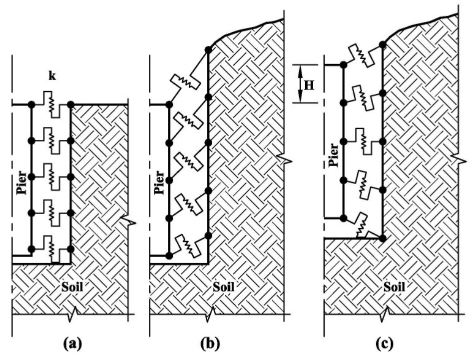

Figure 17. Schematic of pier and soil interface: (a) initial-no force on pier, (b) soil heave-upward force on pier, (c) pier heave-resultant force on pier is zero.

3.3.4 Soil failure and shear strain

If the stress in the soil adjacent to the pier exceeds that which is necessary to cause soil failure by the Mohr-Coulomb theory, and there has been no slip of the soil based on Coulomb friction, the soil will fail in shear and the shear stress on the side of the pier will equal the shear strength of the soil. Loss in soil strength due to strain is incorporated into APEX by a linear decrease in the apparent cohesion and angle of internal friction from their peak values to residual values at a specified shear strain.

Coulomb friction is defined as a linear relationship between normal force and skin friction. The friction is defined by an adhesion factor, α. Benvenga (2005) showed that the value of α can vary widely with most values between about 0.4 to 0.8. Shear strength is defined by the conventional shear strength equation. Figure 18 shows the two relationships.

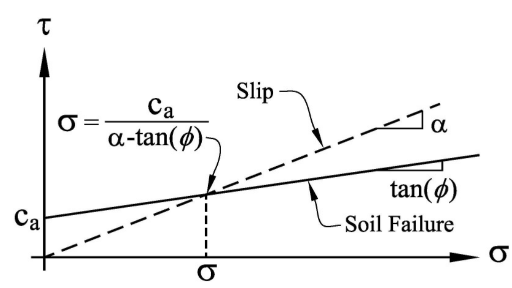

Figure 18. Strength envelopes for slip and soil failure modes

3.3.5 Slip or soil failure

It is not always predictable whether the soil will slip along the pier or failure will occur in the soil. Figure 18 illustrates the allowable shear stress as a function of the normal stress for both mechanisms. Whether one mechanism or the other governs, depends on the normal stress. Thus, it is necessary to monitor both mechanisms throughout the process of iteration.

3.3.6 The iterative process

An iterative solution procedure is used. Simultaneous adjustments are made of the pier heave and the k parameters during each iteration.

3.3.7 Typical APEX results

Typical APEX output is shown in Figure 19 for a soil profile with uniform expansion potential with depth. The cumulative heave profile shown in Figure 19a is the input for the APEX program. Figure 19b shows the distribution of slip along the pier. In this case slip occurred over the entire length. This is reflective of the fact that the shear strength of the soil was sufficiently high that failure occurred as slipping between the pier and the soil at the pier-soil interface. For a soil with a lower shear strength, failure would have occurred in the soil at some distance into the soil away from the interface.

Figure 19c shows the distribution of shear stress along the pier. In the upper portion of the pier the shear stresses are positive. This defines the uplift zone and the lower portion defines the anchorage zone. Figure 19d shows the axial force in the pier. The maximum value occurs at the change from the uplift to the anchorage zone. This is the tensile force in the pier for which the reinforcing steel must be designed.

4. VALIDATION OF THE FINITE ELEMENT BASED ANALYSIS

The APEX code was validated by comparing computed results with field-measured data from project sites where measurements of pier heave or tensile force had been recorded and where reliable soil profile characteristics were available. Two of the validation cases are discussed below. These include a manufacturing building in Colorado, USA, and the Colorado State University Expansive Soil Test Site. The total free-field heave and the distribution of the soil heave with depth was determined using the methods described previously. Details of these case histories are presented in Nelson et al. (2010). Figure 20 shows the calculated soil heave distribution for each case.

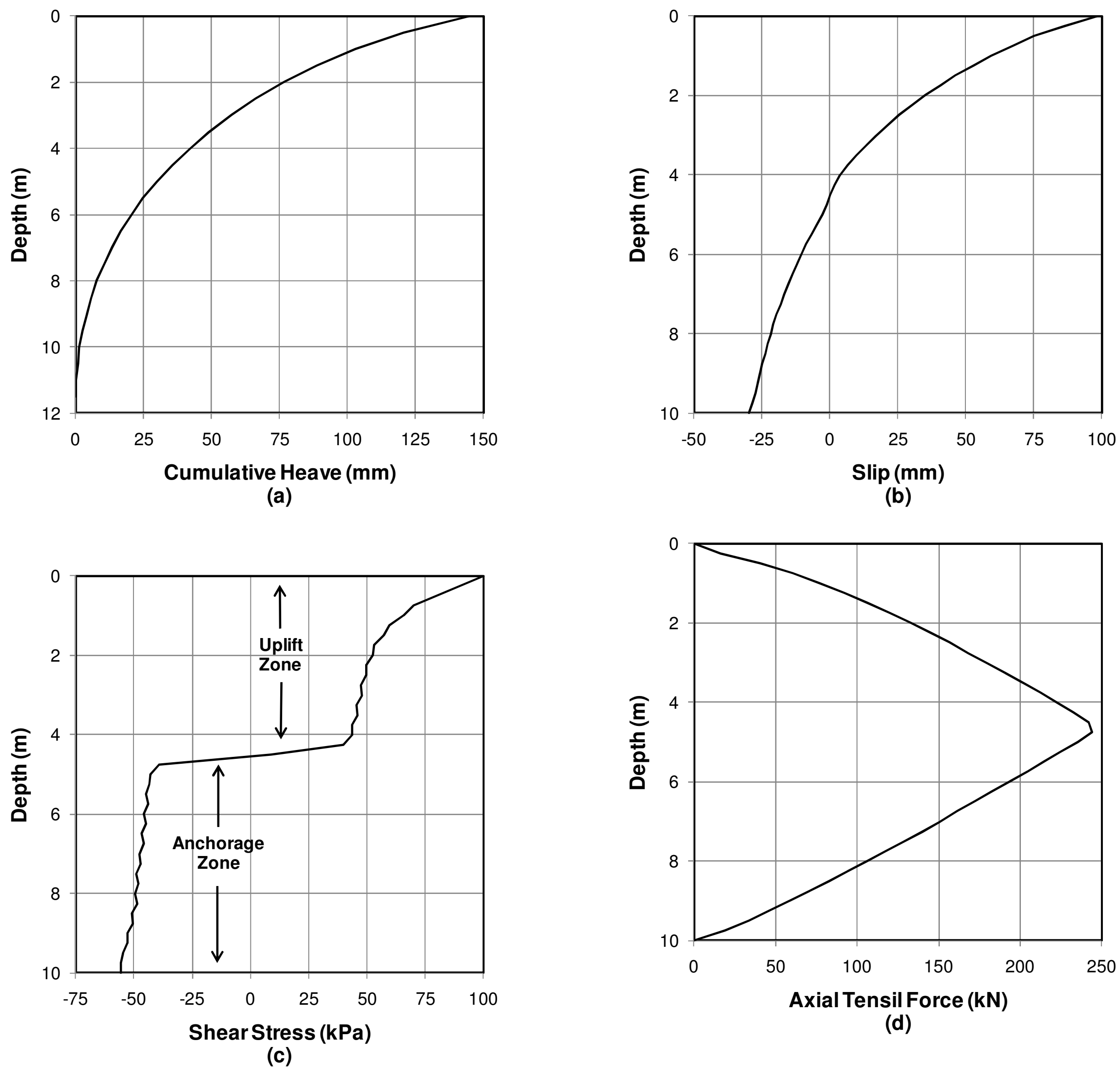

Figure 19 Typical output from APEX Program: (a) cumulative heave used as input, (b) variation of slip along pier, (c) shear stress distribution along pier, (d) axial force distribution.

4.1 Manufacturing Building

The Manufacturing Building is a heavily-loaded concrete and masonry building located on an expansive soil site in Colorado, USA. Structural distress was experienced several years after construction (Attwooll et al., 2006; Overton et al., 2007). The foundation consists of drilled concrete piers having a diameter of 750 mm installed to a depth of 7.0 m. The soil profile at the site consists of approximately 3.8 to 4.3 m of silty/sandy clay underlain by claystone of the Pierre Shale formation. The piers were constructed below the basement level with the top of the piers being about 6 m below the top of original grade. Thus, the piers are located entirely within the Pierre Shale.

The free-field heave profile was calculated for a uniform soil as shown on Figure 20a. Using the APEX code and that heave profile, the ultimate heave of a 750 mm diameter pier with a dead load of 435 kN ranges from 345 to 380 mm for values of E equal to 5,000 kPa and 10,000 kPa, respectively.

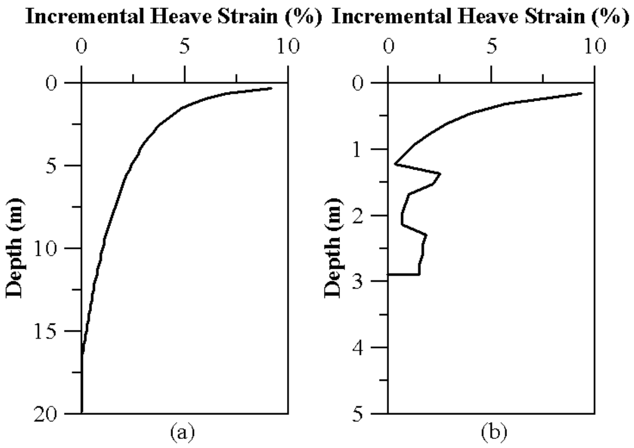

Figure 20 Soil heave profiles for validation cases: (a) Manufacturing Building (b) CSU Test Site

At the time of our investigation the total ultimate pier heave had not yet been realized. The survey data was extended into the future to predict the ultimate pier heave by means of a hyperbolic function.

$$\rho_p = \frac{t}{a+bt} \tag{24}$$

This technique has been used previously for analysis of pier movement in expansive soil (Chao, 2007; Overton et al., 2007). Figure 21 shows the elevation survey data and the hyperbolic function for two groups of piers that experienced large amounts of heave.

The range of values of pier heave calculated using the APEX code is also shown on Figure 21. It is seen that very good agreement exists between the computed value of heave and that determined using measured values.

4.2 CSU Expansive Soil Test Site

The Colorado State University Expansive Soils Test Site is located in an area of the Pierre Shale formation. The soil consists of approximately 0.5 m of organic silt and 0.9-1.2 m of clay underlain by claystone.

Four 350 mm diameter piers were installed at the site to a depth of 7.6 m in August 1995 (Chapel, 1998). Strain gauges were mounted in the center of each pier at depths of 1.8, 3.1, 4.3, and 5.5 m below the ground surface. Irrigation water was placed on the site during summer and fall months during the period from September 1995 through October 1997. The free-field heave adjacent to this example pier was measured to be 64 mm, and the pier heave was 9 mm during the time period from August 1995 to August 1997.

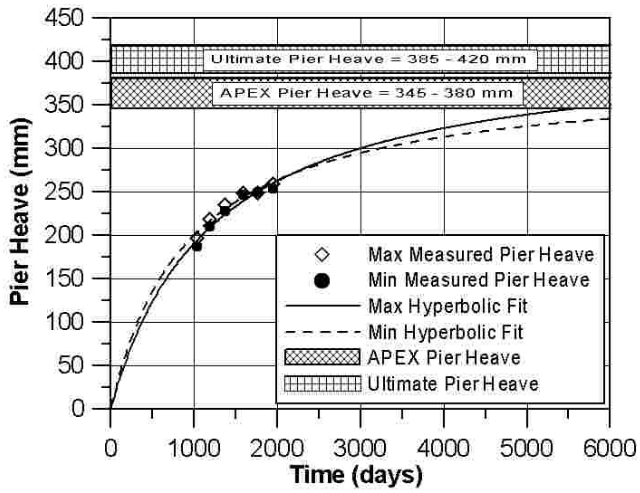

Figure 21 Elevation survey data in hyperbolic form compared with heave computed by APEX for Manufacturing Building

In this case, the APEX model was validated by comparing the measured force in the pier to the force calculated using APEX. Readings taken of the strain gauges in October 1997 were used to calculate the tensile forces in the pier. The total force in the pier was calculated using the values of strain along with the cross-sectional area and modulus of elasticity of the concrete and the steel in the pier.

The measured and computed forces in the pier are shown in Figure 22. There is generally good agreement between the measured and calculated values for the upper three strain gauges.

The high strain gauge reading at a depth of 5.5 m indicates that the concrete at this location was at least partially cracked. For a partially cracked and/or yielded section, the force at that depth would be somewhere between the two values indicated by the solid and open points.

Good agreement is seen between the measured and computed values of force at the upper three strain gauges. The curve falls appropriately between the upper and lower bounds of the measured force at a depth of 5.5 m.

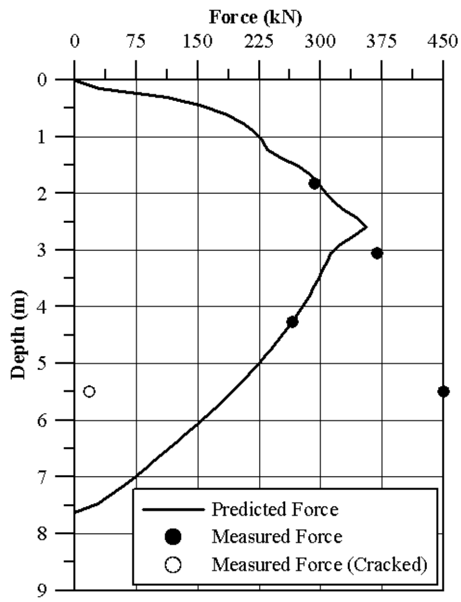

Figure 22 Measured versus predicted axial force in the concrete pier for the CSU Test Site

5. PIER DESIGN CURVES

Curves of the nature shown above in Figures 12 through 15 are being developed using the APEX program for use in facilitating pier design. Concrete piers used in expansive soil applications generally fall within a fairly narrow range of sizes and conditions. The largest diameter drilled concrete piers in expansive soils that the authors have seen are those for the manufacturing building discussed above (750 mm). Most commonly for light one or two story structures, piers with diameters of 250 to 300 mm are used. Micropile diameters are about 100 to 110 mm. Pier lengths of 6 m for the larger diameter piers were common several years ago but they have frequently experienced intolerable heave. Pier lengths in the range of 8 to 12 m are currently common. Micropiles are being used in some instances. The authors are aware of some micropiles as long as 30 m with a diameter of 100 mm being installed. More common micropile lengths are around 15 to 20 m. Thus, common values of L/d range from about 10 to 150. The design charts that are presented below consider the range from 20 to 80 which represents the middle of the range of actual pier sizes.

The design curves presented below were developed for a zero dead load condition. They were developed using a value for the adhesion factor, α, of 0.4. The sensitivity of the results to the α parameter will be discussed at a later point.

Figure 23 shows pier heave normalized with respect to free-field heave as a function of pier length normalized with respect to the depth of the Design Active Zone, Z_{AD}. Figure 24 is an enlargement of that portion of Figure 23 for values of L/Z_{AD} greater than 1.0. This figure facilitates use of the design charts at a larger scale. These figures were prepared for the case where the cumulative free-field heave distribution is linear with depth. This would be the case where the heave for each incremental soil layer, z_i, is the same. The stiffness of the soil is expressed in terms of atmospheres. Thus, $E_A = E_s/1$ atm where E_s is the modulus of elasticity of the soil, and atmospheric pressure is expressed in the same units as E_s.

Figure 25 shows similar curves for the case where the expansion potential of the soil is constant with depth. In that case the cumulative heave profile is non-linear as shown in Figure 25. In Figure 25, it is seen that for L/Z_{AD} less than about 1.5, pier heave is greater for the stiffer soil; whereas the reverse is true for larger values of L/Z_{AD}.

Figure 26 shows the effect of soil stiffness on pier heave. The effect of stiffness is greatest at L/Z_{AD} of 1.3 to 1.5 where the maximum difference is a factor of 1.5 for L/d = 20 and 2 for L/Z_{AD} = 80. At larger values of L/Z_{AD} the stiffer soil exhibits less pier heave than the less stiff soil. This effect of stiffness can be explained by the fact that for the shorter pier the uplift is producing more heave and the stiffer soil in the uplift zone has more influence. For the larger piers, the stiffer soil in the anchorage zone has more influence which then resists the uplift forces.

The effect of stiffness for the nonlinear heave distribution is also plotted on Figure 26 and it is seen that the effect of soil stiffness is very pronounced around values of L/Z_{AD} equal to 1.0. Depending on slenderness ratio, the heave varies by a factor of 2 to 2.7. It is of interest that in Figure 26 the curves for larger values of L/Z_{AD} converge and are less sensitive to the slenderness ratio.

Thus, the stiffness of the soil can have a significant effect on pier heave. This shows the importance of measuring the modulus of elasticity for the soil. The modulus of elasticity can be determined from the slope of the oedometer test results if the soil is assumed to be linearly elastic. However, that would represent the stiffness of a saturated soil. If the foundation soil is not saturated it will be stiffer. For wetting from the surface, Z_A is smaller initially and increases with time. Thus, L/Z_A is large immediately after construction and decreases with time. By the time that the depth of wetting reaches the value of Z_{AD} the soil above the wetting front is wetted and the stiffness is lower. Thus, use of the oedometer test results would be reasonable.

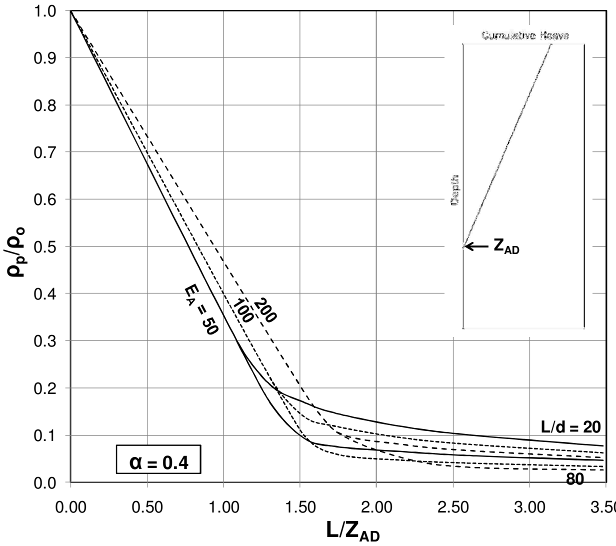

Figure 23 Pier heave as a function of pier length - linear free-field heave distribution

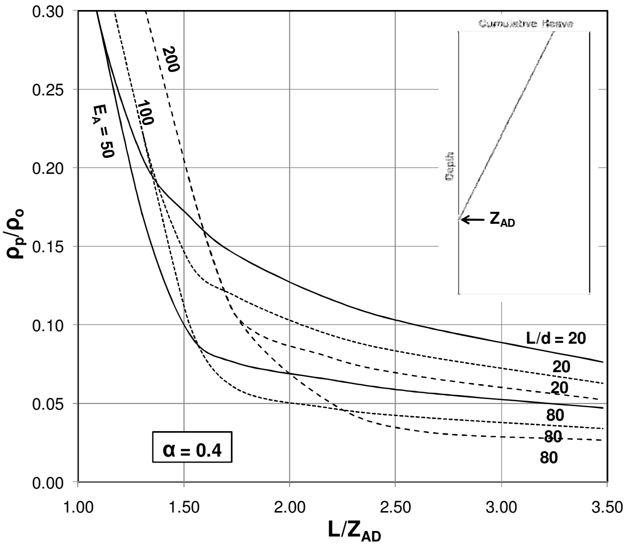

Figure 24 Pier heave for long piers - linear free-field heave distribution

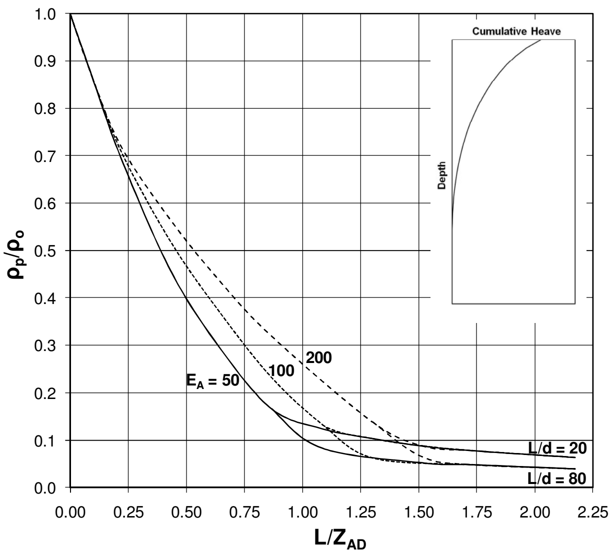

Figure 25 Pier heave as a function of pier length - nonlinear free-field heave distribution

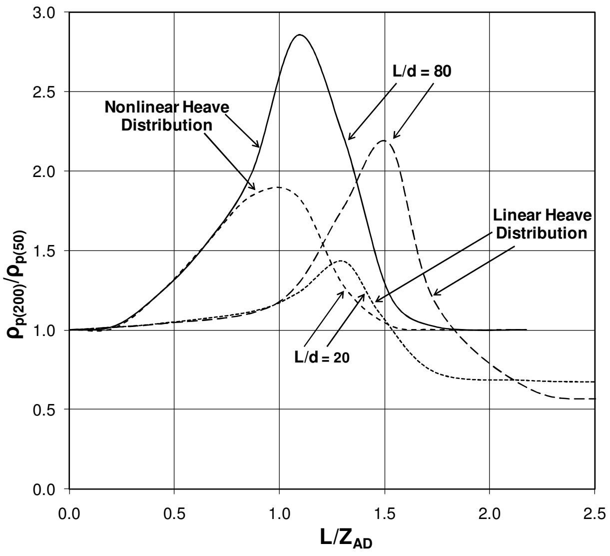

Figure 26 Effect of soil stiffness on pier heave

Figure 27 demonstrates the sensitivity of the pier heave to the value of the adhesion factor, α. In Figure 27a the soil was assumed to have a shear strength such that shear failure would occur in the soil for higher values of α. In Figure 27b the soil shear strength has been assigned a high value such that soil shear failure does not occur for any values of α. In that case the value of α has little or no effect for piers shorter than $1.25\times Z_{AD}$. For longer piers the higher values of α produce greater heave. This implies that the uplift skin friction is producing the greater effect for the longer piers. This is also the case for the soil with the lower shear strength as shown in Figure 27a. In Figure 27a, however, at larger values of α, failure occurs in the soil near the pier-soil interface. The uplift shear stress on the pier is, therefore, lower and the pier heave is lower.

6. EXAMPLE FOUNDATION DESIGN

To demonstrate the use of the design charts that have been presented above, an example calculation was done for a pier and grade beam foundation on a typical soil profile. The soil profile and soil properties are shown in Table 5. This profile is similar to an actual site near Denver, Colorado. The profile at the site consists of 5 m of weathered claystone over unweathered claystone. At a depth of 10 m the claystone became sandy and much less expansive. Based on analyses of ground water migration and the soil profile, the design active zone, Z_{AD}, was taken as 10 m. The free-field heave was computed using Equation (5) and was calculated to be 192 mm. The cumulative heave profile is shown in Figure 28.

For the example calculation, the top of the pier was assumed to be at the ground surface and dead load was neglected. The piers were specified to be straight shaft concrete piers with a diameter of 300 mm, and a tolerable heave of 25 mm. It was assumed that at the end of the design life full wetting will occur throughout the entire depth of potential heave. A value of 0.4 for α was assumed. The required length of pier will be computed using rigid pier, elastic pier and APEX analyses.

6.1 Rigid pier analysis

The required length of a rigid pier is calculated by equating the uplift forces as shown in Figure 11 to the anchorage skin friction forces. The uplift skin friction is equal to

$$f_u = \alpha_1 \sigma'_{cv} \tag{25}$$

Where α_1 is the adhesion factor in the uplift zone. As noted, a value of 0.4 was assumed.

Table 5 Soil properties used in heave calculations for example foundation design

Soil Type	Water Content (%)	Total Density (Mg/m3)	E_s (kPa)	Consolidation-Swell Test (1): Percent Swell (%)	Consolidation-Swell Test (1): Swelling Pressure (kPa)
Weathered Claystone (0–5 m)	12	1.9	9,400	2.0	350
Claystone (5–10 m)	9	1.8	11,200	3.5	550
Sandy Claystone (>10 m)	8	1.8	120,000	1.86	305

(1) Inundation Pressure = 48 kPa

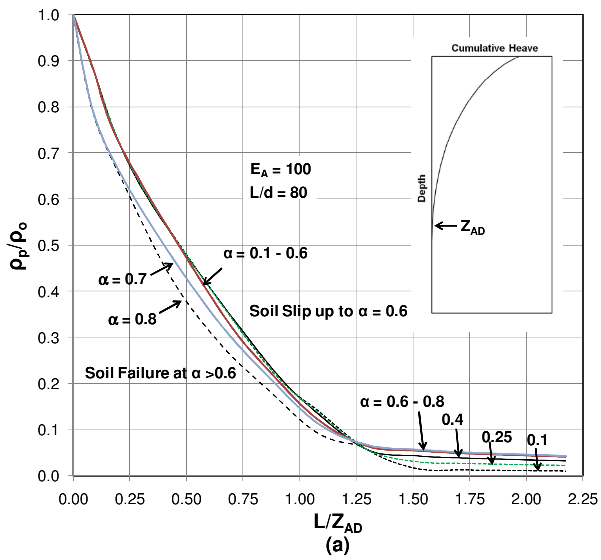

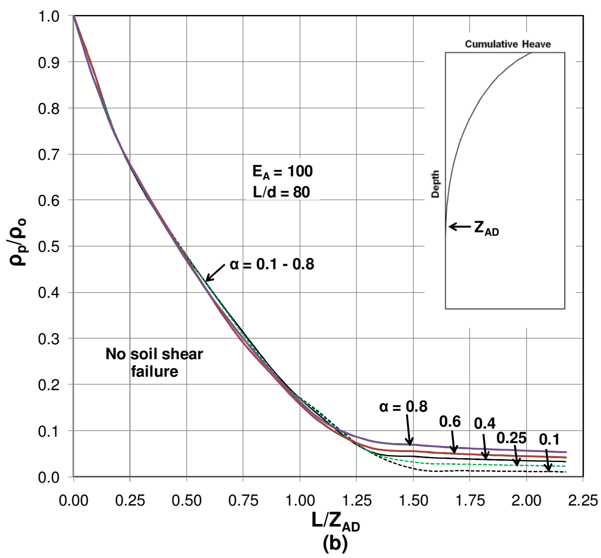

Figure 27. Sensitivity of pier heave to α:
(a) lower soil shear strength allows shear failure,
(b) high soils shear strength forces slip

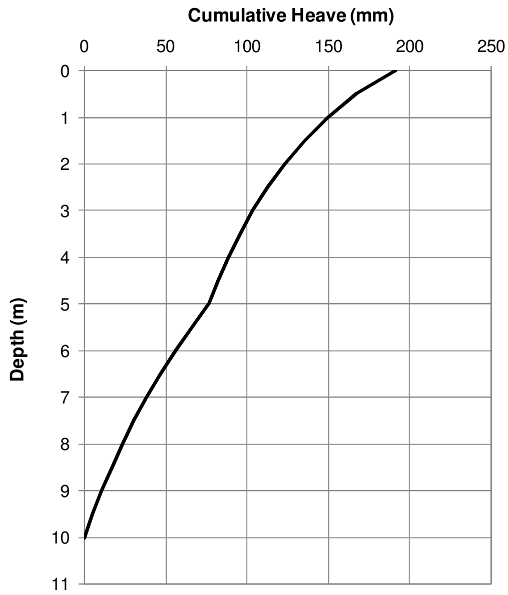

Figure 28. Cumulative heave profile for example calculation

The negative (anchorage) skin friction can be calculated by the equation

$$f_s = \alpha_s \sigma'_h \tag{26}$$

Where α_s is the adhesion factor in the anchorage zone, and σ'_h is the lateral stress acting on the pier. The lateral pressure will be taken as being equal to the constant-volume swelling pressure of the sandy claystone.

The value of α_s should be similar to that of α_1. Therefore, a value of 0.4 was used. The required pier length for a rigid pier was calculated to be 18.7 m.

6.2 Elastic pier analysis

Figure 12 was used to compute the required length of an elastic straight shaft pier. Because the claystone has a high swelling pressure the pier-soil interaction was considered to be constant with depth. This corresponds to case A in Figure 12. The normalized allowable pier heave is

$$\rho_p / \rho = 25.4 / 192 = 0.13 \tag{27}$$

Using case A in Figure 12, at $\rho_p/\rho_o = 0.13$

$$L / Z_{AD} = 1.8 \tag{28}$$

The depth of design active zone, Z_{AD}, was previously determined to be 10 meters. Thus, the required pier length, $L_{req'd}$, is,

$$L_{req'd} = 1.8 \times 10 = 18 \text{ meters} \tag{29}$$

6.3 APEX analysis

The pier design charts shown in Figures 24 and 25 will be used to determine the required pier length. That result will be compared with the value computed using the APEX finite element program directly.

The shape of the cumulative free-field heave curve shown in Figure 28 will dictate whether to use Figure 24 or Figure 25 to represent the actual condition. This example will compare the results from both charts with the results determined directly from the APEX program. The stiffness of the soil averages 10,860 kPa. Since one atmosphere is approximately equal to 100 kPa,

$$E_A = \frac{10{,}860 \text{ kPa}}{100 \text{ kPa}} = 108.6 \tag{30}$$

Therefore, the curve for E_A = 100 in the design charts will be used. From Equation (27), the allowable normalized pier heave is 0.13. At this value, the curves for L/d = 20 and L/d = 80 in Figure 24 diverge and thus, it is necessary to assume a value of L/d in order to use the charts. A value will be estimated and revised if necessary after the required length is computed. The design active zone, Z_{AD}, was computed to be 10 m. If we assume that the pier will be approximately 50% larger than that, L would be 15 m. Thus,

$$\frac{L_{assumed}}{d} = \frac{15 \text{ m}}{0.3 \text{ m}} = 50 \tag{31}$$

As shown on Figure 24, and interpolating between the curves for L/d = 20 and 80,

$$\frac{L_{req'd}}{Z_{AD}} = 1.52 \tag{32}$$

Thus,

$$L_{req'd} = 1.52 \times 10 = 15.2 \text{ m} \tag{33}$$

The initial assumption of L/d = 50 is reasonable and does not need to be refined.

Next it will be assumed that the curve for cumulative heave is non-linear such as that in Figure 25. At a value of $\rho_p/\rho_o = 0.13$, the curves for L/d = 20 and L/d = 50 coincide. Thus, from Figure 25,

$$\frac{L_{req'd}}{Z_{AD}} = 1.10 \tag{34}$$

and

$$L_{req'd} = 1.10 \times 10 = 11.0 \text{ m} \tag{35}$$

These results are compared with the output from the APEX program in Figure 29. As seen from that figure, the results from Figure 24 are the most accurate. It is evident from this example that the shape of the cumulative heave curve can have a significant effect on the results. The curve shown in Figure 28 is nearly linear and the small amount of curvature did not have a major influence.

In some instances, the upper portion of the pier is cased in a material such as PVC in order to reduce the skin friction in the uplift zone. The results from the APEX program from the concrete pier used in this example, but having an upper cased section 6 m long with a value for α = 0.10, are shown also in Figure 29. For that case the required pier length is reduced to 11.4 m. Whether it is more economical to install the sleeved pier or just to drill the pier another 4 m deep is a function of the construction costs. Also the value of α for soil against PVC is closer to 0.3.

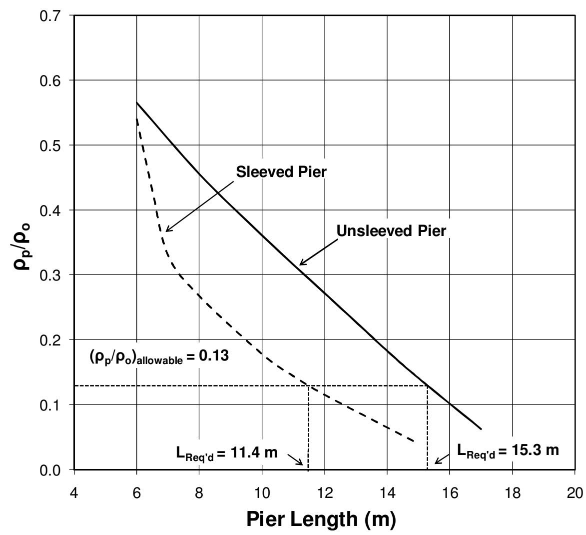

Figure 29. Example pier heave computed from APEX program

7. CONCLUSION

An essential component of the ability of a foundation to provide adequate support of a structure is the expected movement of that foundation. Just as the settlement of a foundation on soft soil must be calculated and analysed, so must the heave of a foundation on expansive soils. This paper has presented the existing state of the art with respect to analysing heave of deep pier foundations in expansive soils. It has presented the design tools that are readily available to the practicing engineers for predicting pier heave, and has presented a rigorous and useful finite element method of analysis. That method has been termed the APEX method.

Prior to development of the APEX method the two most commonly used methods that have been published are the rigid pier method (Chen, 1988) and the elastic pier method (Nelson and Miller, 1992). The rigid pier method assumes equilibrium of the pier, and hence, no pier movement. It provides for an overly conservative design and long pier lengths. The elastic pier method allows for some tolerable amount of pier heave. However, in its currently used form it is limited to use in simplified soil profiles and uniform piers. It has also limitations with respect to the range of slenderness ratios for which it applies.

The APEX program presented in this paper is a more versatile and robust method of analysis, and represents an improvement over the other two methods. It addresses the limitations of those methods and allows for pier analysis within complex soil profiles where soil properties and/or water contents vary with depth. It is also useful for piers with complex construction details such as segmented micropiles.

When compared with the existing rigid and elastic pier analysis methods, APEX generally predicts lower pier heave values when considering a standard straight shaft concrete pier. The magnitude of the difference depends upon the shape of the soil heave profile. It is believed that the APEX method is more realistic and gives more accurate results than the other design methods.

8. REFERENCES

Al-Mhaidib, A. I. (2006). Swelling Behavior of Expansive Shale, a Case Study from Saudi Arabia. Expansive Soils - Recent Advances in Characterization and Treatment. Taylor & Francis Group, London, UK.

Attwooll, B., Reins, J., and Lykosh, P. (2006). Heave at Manufacturing Facility: Observations and Response. Proc. of the 4th Int. Conf. on Unsaturated Soils, April 2-6, 2006, Carefree, Arizona, ASCE Geotechnical Special Publication 147(1), 323-346.

Benvenga, M. M. (2005). Pier-Soil Adhesion Factor for Drilled Shaft Piers in Expansive Soil. M.S. Degree, Colorado State University, Fort Collins, Colorado (J.D. Nelson, advisor).

Bonner, J. P. (1998). Comparison of Predicted Heave Using Oedometer Test Data to Actual Heave. Master's Thesis, Colorado State University, Fort Collins, Colorado.

Chao, K. C. (2007). Design Principles for Foundations on Expansive Soils. Ph.D. Degree, Colorado State University, Fort Collins, Colorado.

Chao, K. C., Overton, D. D., and Nelson, J. D. (2006). The Effects of Site Conditions on the Predicted Time Rate of Heave. American Society of Civil Engineers, Unsaturated Soils Conf. 2006. Special Publication 147, 2086-2097.

Chapel, T. A. (1998). Field Investigation of Helical and Concrete Piers in Expansive Soils. Thesis submitted in partial requirement for the M.S. Degree, Colorado State University, Fort Collins, Colorado.

Chen, F. H. (1988). Foundations on Expansive Soils. Elsevier. New York, NY.

Feng, M., Gan, K-M, and Fredlund, D. G. (1998). A Laboratory Study of Swelling Pressure Using Various Test Methods. Proc. International Conference on Unsaturated Soils, Beijing, China, International Academic Publishers, VI: 350-355. August 27-30.

Fredlund, D. G. (2004). Analysis of Decorah Clay - Shale at the Sandstone Ridge Housing Development in Cannon Falls, Minnesota. Project No. 98823-B. May 20.

GEO-SLOPE International, Ltd. (2007). GEO-STUDIO VADOSE/W Software Package for Seepage Analysis, Version 7.15. Calgary, Alberta, Canada.

Houston, S. L., Houston, W., Zapata, C., and Lawrence, C. (2001). Geotechnical Engineering Practice for Collapsible Soils. Geotechnical and Geological Engineering, Kluwer Academic Publications, 19:333-355.

McWhorter, D. B. and Nelson, J. D. (1979). Unsaturated Flow Beneath Tailings Impoundments. J. Geotech. Eng. Div., ASCE, November, 105(GT11):1317-1334.

Nelson, J. D. (2010). Heave Prediction in Expansive Soils. Panel Discussion, UNSAT 2010, Barcelona, Spain.

Nelson, J. D. and Miller, D. J. (1992). Expansive Soils: Problems and Practice in Foundation and Pavement Design, John Wiley and Sons, New York, NY. USA.

Nelson, J. D., Chao, K. C., and Overton, D. D. (2007). Definition of Expansion Potential for Expansive Soils. Proc. of the 3rd Asian Conf. on Unsaturated Soils. Nanjing, China. 21-23 April. 587-592.

Nelson, J. D., Overton, D. D., and Durkee, D. B. (2001). Depth of Wetting and the Active Zone. Proceedings of the Geo-Institute Shallow Foundation and Soil Properties Committee Sessions at the ASCE 2001 Civil Engineering Conference, Houston, Texas, October.

Nelson, J. D., Reichler, D. K., and Cumbers, J. M. (2006). Parameters for Heave Prediction by Oedometer Tests. Proc. of the 4th Int. Conf. on Unsaturated Soils. Carefree, Arizona. USA. April. ASCE, Geotechnical Special Publication, No. 147: 951-961.

Nelson, J. D., Thompson, E. G., Schaut, R. W., Chao, K. C., Overton, D. D., and Dunham-Friel, J. S. (2010). Design Considerations for Piers in Expansive Soils. ASCE J. Geotech. and Geoenvironmental Engr. (Submitted for publication Sept, 2010).

Overton, D. D., Chao, K. C., and Nelson, J. D. (2006). Time Rate of Heave Prediction for Expansive Soils. American Society of Civil Engineers, Proc. of GeoCongress 2006 Conf. Atlanta. February.

Overton, D. D., Chao, K. C., and Nelson, J. D. (2007). Heave Distress of a Manufacturing Building. Proc. of the Geo-Denver 2007 Conf., Denver. February. In Contemporary Issues in Deep Foundations (GSP 158).

Porter, A. (1977). The Mechanics of Welling in Expansive Clays. Master of Science Thesis, Colorado State University, Fort Collins, Colorado.

Poulos, H. G. and Davis, E. H. (1980). Pile Foundation Analysis and Design. John Wiley, New York. USA.

Reichler, D. K. (1997). Investigation of Variation in Swelling Pressure Values for an Expansive Soil. Thesis submitted in partial requirement for the Master Degree, Colorado State University, Fort Collins, Colorado.

Thompson, R. W., Perko, H. A., and Rethamel, W. D. (2006). Comparison of Constant Volume Swell Pressure and Oedometer Load-Back Pressure. Proceedings of the Fourth International Conference on Unsaturated Soils. Carefree, Arizona. April, 1787 – 1798.

Washington State University. (2002). Biological Systems Engineering Department, ClimGen – Climate Data Generator Users Manual, Pullman, Washington.